Nonadiabatic Dynamics within Time-Dependent Density Functional Tight Binding Method†

Roland Mitrić,*,§ Ute Werner,‡ Matthias Wohlgemuth,‡ Gotthard Seifert,¶ and Vlasta Bonačić-Koutecký*,‡

Fachbereich Physik, Freie Universität Berlin, Arnimallee 14, D-14195 Berlin, Germany, Institut für Chemie, Humboldt-Universität zu Berlin, Brook-Taylor-Strasse 2, D-12489 Berlin, Germany, and Physikalische Chemie, Technische Universität Dresden, D-01062 Dresden, Germany

Received: June 15, 2009; Revised Manuscript Received: July 28, 2009

A nonadiabatic molecular dynamics is implemented in the framework of the time-dependent density functional tight binding method (TDDFTB) combined with Tully's stochastic surface hopping algorithm. The applicability of our method to complex molecular systems is illustrated on the example of the ultrafast excited state dynamics of microsolvated adenine. Our results demonstrate that in the presence of water, upon initial excitation to the S_3 ($\pi-\pi^*$) state at 260 nm, an ultrafast relaxation to the S_1 state with a time constant of 16 fs is induced, followed by the radiationless decay to the ground state with a time constant of 200 fs.

Introduction

The ultrafast molecular dynamics in the excited electronic states is characterized by nonadiabatic processes in which the coupling between nuclear and electronic motion leads to nonradiative transitions between electronic states. Such nonradiative transitions are responsible for fundamental photochemical processes such as internal conversion, isomerization, electron transfer, proton transfer, and so forth[1−4] which are ubiquitous in photochemistry. The theoretical exploration of coupled electron−nuclear dynamics in complex molecular systems requires the development of accurate and efficient methods for the simulation of nonadiabatic dynamics. One of the most efficient approaches is based on the mixed quantum−classical dynamics, in which the nuclear motion is described by classical trajectories propagated using quantum chemical ab initio molecular dynamics "on the fly", combined with the stochastic Tully's surface hopping (TSH) procedure[5] for the description of nonadiabatic electronic transitions. The forces and nonadiabatic couplings needed to propagate classical nuclear trajectories can be obtained using the whole spectrum of methods such as ab initio "frozen ionic bond" approximation,[6] ab initio configiration interaction (CI),[7] restricted open−shell Kohn−Sham density functional theory (DFT),[8] linear response time-dependent density functional theory (TDDFT),[9−13] as well as semiempirical methods for the electronic structure.[14−17] In particular, the TDDFT represents an efficient, generally applicable method for the treatment of the optical properties in complex systems, and its performance and accuracy have been steadily improved.[18] Therefore, a variety of methods for nonadiabatic dynamics in the framework of TDDFT have been developed and successfully applied.[8−13]

A particularly attractive possibility to extend the applicability of the TDDFT nonadiabatic dynamics to even larger systems such as biomolecules interacting with the environment or complex nanostructures is to use the approximate tight binding density functional theory (DFTB).[19−22] The self−consistent DFTB has been shown to provide a quite accurate description of ground state properties such as molecular geometries, vibrational frequencies, and reaction energies.[23] Furthermore, the time-dependent linear response formalism[24] and analytic energy derivatives have been implemented in the framework of DFTB,[25] allowing for the description of the optical response of complex molecular systems. The comparison of the accuracy of the TDDFTB approach with full TDDFT shows a very good agreement for singlet electronic states, while the performance of TDDFTB for triplet states shows slightly larger systematic error.[26] It should be noted that while TDDFTB reproduces the accuracy of the TDDFT method, it also shares all of its deficiencies, such as the inability to describe accurately excited states with long range charge transfer character or excited states with significant contribution of double or higher electron excitations. However, despite these drawbacks, the TDDFTB method combined with nonadiabatic dynamics provides an efficient method for the simulation of ultrafast excited state processes in complex systems including their environment. For example, the inclusion of the solvent effects in the excited state dynamics of biochromophores is of particular importance since the presence of the solvent can change both stationary optical properties as well as the mechanism and the time scales of the nonradiative relaxation processes. Recently, the excited state properties of solvated DNA nucleobases have been investigated in the framework of TDDFT combined with the polarized continuum model.[27,28] These studies have revealed that the presence of water can reverse the ordering of the $\pi-\pi^*$ and $n-\pi^*$ states in uracil, leading to different mechanisms for the nonradiative relaxation.[27] However, the realistic picture of the nonadiabatic dynamics of solvated biochromophores can only be obtained if at least a part of the solvent from the first solvation shell is explicitly included in the dynamical simulations.

The ultrafast dynamics of DNA bases has been intensively studied in recent years in order to reveal molecular features which are responsible for their intrinsic photostability.[29] In the case of adenine, experimental studies have shown that isolated adenine in the gas phase returns nonradiatively to the ground state within about 1 ps after photoexcitation of the strongly absorbing $\pi-\pi^*$ electronic state.[30−32] In order to identify the

† Part of the "Russell M. Pitzer Festschrift".

* To whom correspondence should be addressed. E-mail: mitric@zedat.fu-berlin.de (R.M.); vbk@chemie.hu-berlin.de (V.B.K.).

§ Freie Universität Berlin.

‡ Humboldt-Universität zu Berlin.

¶ Technische Universität Dresden.

10.1021/jp905600w CCC: $40.75
Published on Web 08/24/2009

mechanism of the nonradiative relaxation, several theoretical studies have been performed with the aim to assign the conical intersections which dominate the relaxation process.[33−36] Recently, mixed quantum−classical dynamics simulations, both using high−level ab initio multireference CI[37] as well as semiempirical CI,[15] have been performed, giving a dynamical picture of the relaxation process. According to these studies, the relaxation proceeds in a two−step mechanism. First, the initially excited S_3 state relaxes via the S_2 state to the lowest S_1 excited state with a time constant of 22 fs. The second, slower step corresponds to the transiton from the S_1 state to the electronic ground state with a time constant of about 500 fs.

A fundamental issue in the photophysics of nucleobases is the role played by water. The experimental study of adenine in solution[38] using femtosecond transient absorption spectrocopy has revealed that the lifetime of the S_1 state of adenine in water of 180 fs is 50−100% shorter than that in acetonitrile (440 fs) and is, in general, much shorter than that in the gas phase (1.2 ps).[32] This shows that the realistic description of nucleobase dynamics requires the explicit inclusion of solvent effects, which is a challenging task from the theoretical point of view. We show in this paper that the TDDFTB nonadiabatic dynamics represents a general and highly efficient method which can be used to simulate the nonadiabatic dynamics of biochromophores solvated by a large number of water molecules which are not accessible to high−level ab initio methods. Due to its accuracy, which is comparable to that of the full TDDFT method, TDDFTB nonadiabatic dynamics can be used to investigate nonadiabatic processes in a whole variety of complex systems, such as solvated biochromophores, photoreceptors, or nanostructures, which are of interest for material science applications.

In this paper, we present the formulation of nonadiabatic dynamics in the framework of the tight binding time−dependent density functional theory combined with the TSH method. As an illustration of the applicability of our method to large systems of biological relevance, we have chosen to study the ultrafast nonradiative relaxation of the microsolvated DNA base adenine.

The paper is structured as follows: In the Theoretical Formulation section, the theoretical approach is outlined. Subsequently, in the Results and Discussion, we present the application of the method to the ultrafast excited state dynamics of microsolvated adenine. Finally, the conclusions and outlook are given.

Theoretical Formulation

The theoretical formulation of the nonadiabatic dynamics "on the fly" in the framework of the TDDFTB method combined with Tully's surface hopping method is conceptually similar to the one presented previously for the full TDDFT method.[11,12] In this approach, the electronic wave function is represented in the basis of adiabatic Born−Oppenheimer states, which are parametrically dependent on the classical nuclear trajectory $\mathbf{R}(t)$ according to

$$|\Psi(\mathbf{r};\mathbf{R}(t))\rangle = \sum_K C_K(t)|\Psi_K(\mathbf{r};\mathbf{R}(t))\rangle \tag{1}$$

where $|\Psi_K(\mathbf{r};\mathbf{R}(t))\rangle$ represents the adiabatic electronic state K while the $C_K(t)$ are the time-dependent expansion coefficients. The nuclear trajectories $\mathbf{R}(t)$ are obtained by solving the classical Newton's equations of motion. The time evolution of the coefficients $C_K(t)$ along a given classical trajectory can be obtained by solving the time-dependent Schrödinger equation

$$i\hbar\frac{dC_K(t)}{dt} = E_K C_K(t) - i\hbar\sum_I \left\langle \Psi_K(\mathbf{r};\mathbf{R}(t))\middle|\frac{\partial\Psi_I(\mathbf{r};\mathbf{R}(t))}{\partial t}\right\rangle C_I(t) \tag{2}$$

where E_K represents the energy of the electronic state K and the second term corresponds to the nonadiabatic coupling D_{KI} between the states I and K. The latter can be approximately calculated using the finite difference approximation for the time derivative

$$D_{KI}\left(\mathbf{R}\left(t+\frac{\Delta}{2}\right)\right) \approx \frac{1}{2\Delta}(\langle\Psi_K(\mathbf{r};\mathbf{R}(t))|\Psi_I(\mathbf{r};\mathbf{R}(t+\Delta))\rangle - \langle\Psi_K(\mathbf{r};\mathbf{R}(t+\Delta))|\Psi_I(\mathbf{r};\mathbf{R}(t))\rangle) \tag{3}$$

where Δ is the time step used for the integration of the classical Newton's equations of motion.

The time−dependent coefficients $C_K(t)$, which are obtained by the numerical solution of eq 2, can be used to calculate the hopping probabilities P_{KI} needed for switching the trajectory between the electronic states in the framework of the TSH procedure. In our approach (cf. ref 12), we calculate the hopping probabilities at each time−step during the integration of eq 2 according to

$$P_{KI}(\tau) = -2\frac{\Delta\tau[\mathrm{Re}(C_K^*(\tau)C_I(\tau)D_{KI}(\tau))]}{C_K(\tau)C_K^*(\tau)} \tag{4}$$

The $\Delta\tau$ represents the time−step used for the numerical integration of eq 2 for the electronic state coefficients and is typically much smaller than the nuclear time−step Δ.

The nonadiabatic coupling D_{KI} together with the forces acting on the nuclei in the excited electronic states are the essential quantities needed to perform the nonadiabatic dynamics simulations and are calculated in the framework of the TDDFTB method. In the following, we will give a short outline of the TDDFTB method with the emphasis on the calculation of the nonadiabatic couplings.

(i) Nonadiabatic Coupling within the Linear Response TDDFTB Method. The essential idea of the DFTB method is to perform a second-order perturbation expansion of the DFT total energy functional around the given reference density $\rho_0(\mathbf{r})$[21]

$$E = \sum_i^{\mathrm{occ}} n_i\langle\phi_i|\hat{H}^0|\phi_i\rangle + \frac{1}{2}\int\int f_{\mathrm{xc}}[\mathbf{r},\mathbf{r}']\delta\rho\delta\rho' - \frac{1}{2}\int\int\frac{\rho_0(\mathbf{r})\rho_0(\mathbf{r}')}{|\mathbf{r}-\mathbf{r}'|} + E_{\mathrm{xc}}[\rho_0] - \int V_{\mathrm{xc}}[\rho_0]\rho_0 + E_{ii} \tag{5}$$

where $\hat{H}^0$ is the Kohn−Sham Hamiltonian evaluated at the reference density, ϕ_i are the Kohn−Sham (KS) orbitals, n_i are the occupation numbers, $f_{\mathrm{xc}}[\mathbf{r},\mathbf{r}']$ is the Coulomb exchange−correlation kernel

$$f_{\mathrm{xc}}[\mathbf{r},\mathbf{r}'] = \frac{1}{|\mathbf{r}-\mathbf{r}'|} + \frac{\delta^2 E_{\mathrm{xc}}}{\delta\rho\delta\rho'} \tag{6}$$

and E_{xc}, V_{xc}, and E_{ii} represent the exchange−correlation energy and potential and the core−core repulsion, respectively. The second−order term in eq 5 is decomposed in atom−centered monopol contributions of the form

$$\frac{1}{2}\sum_{AB}^{N}\Delta q_A \gamma_{AB}\Delta q_B \tag{7}$$

where Δq_A represents the Mulliken charge on atom A and γ_{AB} is defined as

$$\gamma_{AB} = \int\int f_{\mathrm{xc}}[\mathbf{r},\mathbf{r}']F_A(\mathbf{r})F_B(\mathbf{r}') \tag{8}$$

with $F_A(\mathbf{r})$ representing a normalized spherical density distribution on atom A. The effective Hamiltonian $\hat{H}^0$ in eq 5 is represented in a minimal basis set using only valence atomic orbitals, and the reference electron density ρ_0 is given as a superposition of atomic densities. Thus, the diagonal elements correspond to the atomic KS eigenvalues, and the nondiagonal elements are calculated in a two-center approximation

$$H^0_{\mu,\nu} = \langle\phi_\mu|\hat{T} + V_{\mathrm{eff}}[\rho^0_A + \rho^0_B]|\phi_\nu\rangle \tag{9}$$

where ϕ_μ and ϕ_ν denote the atomic KS orbitals and $\hat{T}$ and V_{eff} represent the kinetic energy operator and the effective KS potential, respectively. Therefore, within the DFTB approximation, the total energy functional reads

$$E = \sum_{i}^{\mathrm{occ}} n_i \sum_{\mu\nu} c^i_\mu H^0_{\mu,\nu} c^i_\nu + \frac{1}{2}\sum_{AB}\Delta q_A \gamma_{AB}\Delta q_B + E_{\mathrm{rep}} \tag{10}$$

with the effective ion−ion repulstion E_{rep}. By applying the variation principle to this energy functional (eq 10), a generalized eigenvalue problem is obtained

$$\sum_{\nu}(H_{\mu\nu} - \varepsilon_i S_{\mu,\nu})c^i_\nu = 0 \qquad \forall i, \forall\mu \tag{11}$$

where c^i_ν and ε_i represent the KS molecular orbital coefficients and KS orbital energies and $H_{\mu\nu}$ is defined as

$$H_{\mu\nu} = H^0_{\mu\nu} + \frac{1}{2}S_{\mu\nu}\sum_{C}(\gamma_{AC} + \gamma_{BC})\Delta q_C \tag{12}$$

where $S_{\mu\nu}$ represents the overlap matrix. The computational efficiency of the DFTB approach is based on the fact that all necessary matrix elements are tabulated as functions of the interatomic distance based on ab initio DFT calculations and no integral evaluation is necessary.

In analogy with the full TDDFT formalism, the excitation energies ω within the TDFTB method can be obtained as the solution of the eigenvalue problem

$$\begin{bmatrix} A & B \\ B^* & A^* \end{bmatrix}\begin{bmatrix} X \\ Y \end{bmatrix} = \omega\begin{bmatrix} I & 0 \\ 0 & -I \end{bmatrix}\begin{bmatrix} X \\ Y \end{bmatrix} \tag{13}$$

where A and B represent matrices with the elements given by

$$A_{ia,jb} = (\varepsilon_a - \varepsilon_i)\delta_{ij}\delta_{ab} + 2K_{ia,jb} \tag{14}$$

$$B_{ia,jb} = 2K_{ia,jb} \tag{15}$$

and indices i,j and a,b label the occupied and virtual KS orbitals with energies ε_i and ε_a, respectively. The coupling matrix elements $K_{ia,jb}$ can be calculated in the framework of TDDFTB using the generalized Mulliken approximation to the transition densities and have the following form

$$K_{ia,jb} = \sum_{AB} q^{ia}_A \gamma_{AB} q^{jb}_B \tag{16}$$

Notice, that the form of the coupling matrix element is consistent with the monopol approximation for the exchange−correlation kernel F_{xc} in the ground state, and its evaluation also does not require the integral calculation, which makes the TDDFTB calculations highly efficient.[22]

In order to calculate the nonadiabatic couplings in the framework of the TDDFTB method, we use an ansatz for the excited state electronic wave function in terms of singly excited configurations from the manifold of occupied KS orbitals to virtual KS orbitals

$$|\Psi_K(\mathbf{r};\mathbf{R}(t))\rangle = \sum_{i,a} c^K_{i,a}|\Phi^{\mathrm{CSF}}_{i,a}(\mathbf{r};\mathbf{R}(t))\rangle \tag{17}$$

where $c^K_{i,a}$ represents the CI coefficients and $|\Phi^{\mathrm{CSF}}_{i,a}(\mathbf{r};\mathbf{R}(t))\rangle$ is the singlet spin−adapted configuration state function (CSF) defined as

$$|\Phi^{\mathrm{CSF}}_{i,a}(\mathbf{r};\mathbf{R}(t))\rangle = \frac{1}{\sqrt{2}}(|\Phi^{a\beta}_{i\alpha}(\mathbf{r};\mathbf{R}(t))\rangle + |\Phi^{a\alpha}_{i\beta}(\mathbf{r};\mathbf{R}(t))\rangle) \tag{18}$$

with $|\Phi^{a\beta}_{i\alpha}(\mathbf{r};\mathbf{R}(t))\rangle$ and $|\Phi^{a\alpha}_{i\beta}(\mathbf{r};\mathbf{R}(t))\rangle$ representing Slater determinants with single excitations from occupied orbital i to virtual orbital a with spin α or β, respectively.

As shown previously,[11,12] for nonhybrid functionals without exact exchange contribution, the CI coefficients $c^K_{i,a}$ giving rise to mutually orthogonal electronic states can be calculated from the eigenvectors of eq 13 and are given by

$$c^K_{i,a} = (\varepsilon_a - \varepsilon_i)^{-1/2}(X_{ia} + Y_{ia}) \tag{19}$$

In order to calculate the nonadiabatic couplings according to the discrete approximation in eq 3, the overlap between two CI wave functions at times t and $t + \Delta$ is needed

$$\langle\Psi_K(\mathbf{r};\mathbf{R}(t))|\Psi_I(\mathbf{r};\mathbf{R}(t+\Delta))\rangle = \sum_{ia}\sum_{i'a'} c^{*K}_{i,a}c^I_{i',a'}\langle\Phi^{\mathrm{CSF}}_{i,a}(\mathbf{r};\mathbf{R}(t))|\Phi^{\mathrm{CSF}}_{i',a'}(\mathbf{r};\mathbf{R}(t+\Delta))\rangle \tag{20}$$

The overlap of the CSFs in eq 20 can be reduced to the overlap of singly excited Slater determinants using eq 18, which can be further reduced to the overlap of spatial KS orbitals $\phi_i(t)$ and $\phi'_{i'}(t+\Delta)$ at time steps t and $t+\Delta$

$$\langle \Phi_{i,a}^{\mathrm{CSF}}(\mathbf{r};\mathbf{R}(t))|\Phi_{i',a'}^{\mathrm{CSF}}(\mathbf{r};\mathbf{R}(t+\Delta))\rangle = \begin{bmatrix} \langle\phi_1|\phi'_1\rangle & \cdots & \langle\phi_1|\underline{\phi'_{i'}}\rangle & \cdots & \langle\phi_1|\phi'_n\rangle \\ \vdots & & \vdots & & \vdots \\ \langle\underline{\phi_i}|\phi'_1\rangle & \cdots & \langle\underline{\phi_i}|\underline{\phi'_{i'}}\rangle & \cdots & \langle\underline{\phi_i}|\phi'_n\rangle \\ \vdots & & \vdots & & \vdots \\ \langle\phi_n|\phi'_1\rangle & \cdots & \langle\phi_n|\underline{\phi'_{i'}}\rangle & \cdots & \langle\phi_n|\phi'_n\rangle \end{bmatrix} \begin{bmatrix} \langle\phi_1|\phi'_1\rangle & \cdots & \langle\phi_1|\underline{\phi'_{a'}}\rangle & \cdots & \langle\phi_1|\phi'_n\rangle \\ \vdots & & \vdots & & \vdots \\ \langle\underline{\phi_a}|\phi'_1\rangle & \cdots & \langle\underline{\phi_a}|\underline{\phi'_{a'}}\rangle & \cdots & \langle\underline{\phi_a}|\phi'_n\rangle \\ \vdots & & \vdots & & \vdots \\ \langle\phi_n|\phi'_1\rangle & \cdots & \langle\phi_n|\underline{\phi'_{a'}}\rangle & \cdots & \langle\phi_n|\phi'_n\rangle \end{bmatrix} + \begin{bmatrix} \langle\phi_1|\phi'_1\rangle & \cdots & \langle\phi_1|\underline{\phi'_{a'}}\rangle & \cdots & \langle\phi_1|\phi'_n\rangle \\ \vdots & & \vdots & & \vdots \\ \langle\underline{\phi_i}|\phi'_1\rangle & \cdots & \langle\underline{\phi_i}|\underline{\phi'_{a'}}\rangle & \cdots & \langle\underline{\phi_i}|\phi'_n\rangle \\ \vdots & & \vdots & & \vdots \\ \langle\phi_n|\phi'_1\rangle & \cdots & \langle\phi_n|\underline{\phi'_{a'}}\rangle & \cdots & \langle\phi_n|\phi'_n\rangle \end{bmatrix} \begin{bmatrix} \langle\phi_1|\phi'_1\rangle & \cdots & \langle\phi_1|\underline{\phi'_{i'}}\rangle & \cdots & \langle\phi_1|\phi'_n\rangle \\ \vdots & & \vdots & & \vdots \\ \langle\underline{\phi_a}|\phi'_1\rangle & \cdots & \langle\underline{\phi_a}|\underline{\phi'_{i'}}\rangle & \cdots & \langle\underline{\phi_a}|\phi'_n\rangle \\ \vdots & & \vdots & & \vdots \\ \langle\phi_n|\phi'_1\rangle & \cdots & \langle\phi_n|\underline{\phi'_{i'}}\rangle & \cdots & \langle\phi_n|\phi'_n\rangle \end{bmatrix} \tag{21}$$

The underlined orbitals label the replacement of an occupied orbital by a virtual orbital such as $i \rightarrow a$ and $i' \rightarrow a'$ at t and $t + \Delta$, respectively. The spatial KS overlap integrals can be further reduced to the overlap integrals involving atomic basis functions $b_k(t)$ and $b'_m(t + \Delta)$ and the MO coefficients $c_{ik}(t)$ and $c'_{jm}(t + \Delta)$

$$\langle \phi_i(t)|\phi'_{j'}(t+\Delta)\rangle = \sum_{k=1}^{n}\sum_{m=1}^{n} c_{ik}(t)c'_{jm}(t+\Delta) \times \langle b_k(\mathbf{R}(t))|b'_m(\mathbf{R}(t+\Delta))\rangle \tag{22}$$

The two sets of basis functions $b_k(\mathbf{R}(t))$ and $b'_m(\mathbf{R}(t + \Delta))$ are centered at different positions $\mathbf{R}(t)$ and $\mathbf{R}(t + \Delta)$ and therefore do not form an orthonormal basis set. In order to calculate such overlap matrix elements in the framework of the DFTB approach, the calculation of the overlap matrix $S_{\mu\nu}$ has to be extended from the usual range which covers the region of typical atom−atom distances to the range of very small distances.

Results and Discussion

In order to illustrate the applicability of our TDDFTB nonadiabatic dynamics for the investigation of complex systems, we present here the simulation of the nonadiabatic relaxation of microsolvated adenine. From the experimental work in water solution, it is known that adenine in water assumes two tautomeric forms termed 9H−adenine and 7H−adenine.[38] However, since 9H−adenine is the dominant form (∼78%) that exhibits ultrafast excited state relaxation, we limit ourselves here only to the study of its photodynamics. Our system consists of the adenine molecule solvated by 26 water molecules. The initial structure was prepared in several steps, starting with the equilibration of a water box consisting of 561 water molecules with 30 Å × 30 Å × 30 Å dimensions using constant-temperature molecular dynamics at $T = 300$ K and the TIP−3P force field.[39] After equilibration, the adenine molecule was inserted in the center of the water box and further equilibrated by using the AMBER force field[40] for adenine. Subsequently, the first solvation shell was isolated and optimized by using the B3LYP functional[41] combined with the triple-ζ valence plus polarization basis set (TZVP)[42] as well as by using the DFTB method. The optimized structure of microsolvated adenine presented in Figure 1 shows that all nitrogen atoms of adenine as well as the two hydrogen atoms of the amino group are saturated by hydrogen bonds.

In order to check the accuracy of the TDDFTB method, the absorption spectrum for the B3LYP-optimized structure has been calculated both at the B3LYP/TZVP level as well as by using TDDFTB. The comparison of the absorption spectra in Figure 2 demonstrates a qualitative agreement between the full TDDFT and TDDFTB spectra and gave us confidence to carry out the nonadiabatic dynamics simulations in the framework of TD-DFTB. The first intense transition in TDDFT located at around 250 nm (cf. red arrow in Figure 2a) corresponds to the $\pi-\pi^*$ transition within adenine. The analogous transition in TDDFTB is located at around 260 nm (cf. Figure 2b). While the position of the $\pi-\pi^*$ in both methods is very similar, the $n-\pi^*$ transition within the B3YLP method is located at 240 nm above the $\pi-\pi^*$, but in TDDFTB, the $n-\pi^*$ transition is very close to the $\pi-\pi^*$ one and is located at 268 nm. In fact, the relative position of the $n-\pi^*$ and $\pi-\pi^*$ transition within TDDFTB is analogous to the one found using the ab initio multireference perturbation configuration interaction method (CIPSI) combined with the PCM−IEF solvation model.[43]

In order to study the photodynamics of microsolvated adenine, 100 initial conditions have been sampled from a 10 ps classical trajectory at $T = 300$ K. The trajectories have been propagated using our TDDFTB nonadiabatic dynamics starting in the third excited state S_3. Totally, seven excited states and the ground electronic state have been included in the simulation. The time-dependent excited state populations obtained from the ensemble of 100 trajectories are shown in Figure 3. The initially populated

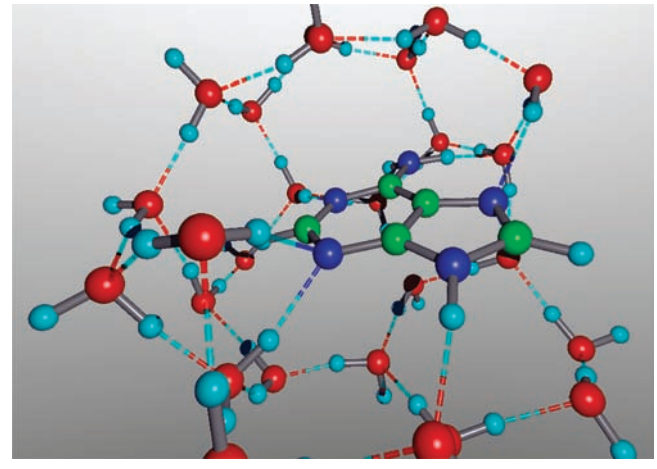

Figure 1. The DFT/B3LYP-optimized structure of microsolvated adenine.

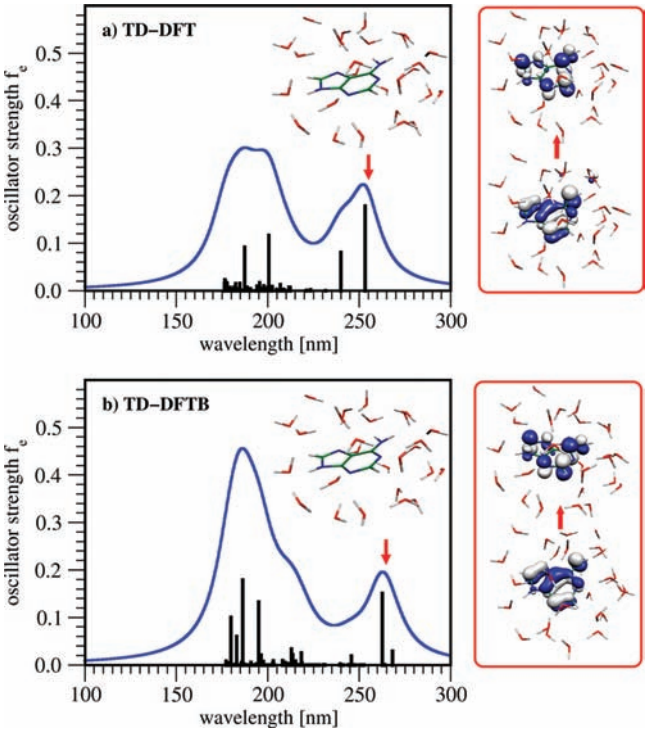

Figure 2. Comparison of the absorption spectra of microsolvated adenine obtained using (a) full TDDFT with the hybrid B3LYP functional and (b) the TDDFTB method. The inset shows the B3LYP/TZVP-optimized structure used for spectrum calculation. The right panels show the character of the main excitation contributing to the first intense transition marked by red arrows.

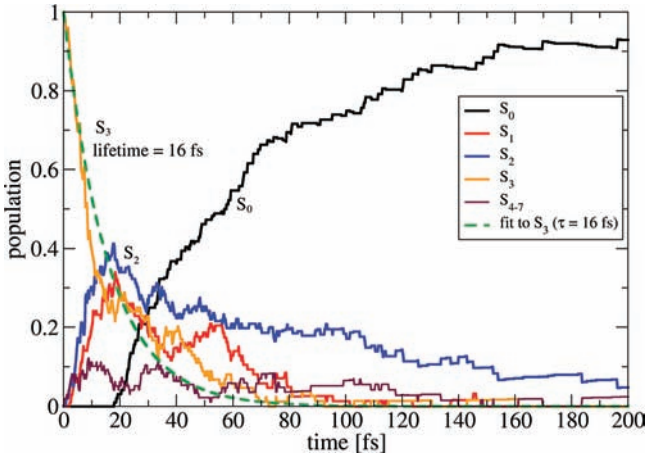

Figure 3. Population of the ground and excited electronic states during the nonadiabatic dynamics simulation for microsolvated adenine.

S_3 state is depopulated with the time constant of 16 fs, and the population is transiently transferred to the lower-lying S_2 and S_1 states as well as, to a lesser extent, to several other energetically close−lying states (S_4−S_7). Notice that no direct population transfer from the initially occupied S_3 state to the ground electronic state occurs. The S_0 state begins to be continuously populated from the S_2 and S_1 states starting at ∼20 fs, with the full population transfer occurring on the time scale of 200 fs. It should be emphasized that the nonadiabatic dynamics of the microsolvated adenine is qualitatively similar to the one of the isolated adenine simulated by using both the high-level ab initio CI method[37] and the semiempirical CI method.[15] However, the transition to the electronic ground state in microsolvated adenine is significantly faster than that in the gas phase (200 fs versus ∼550 fs[15,37]). Notice that previously

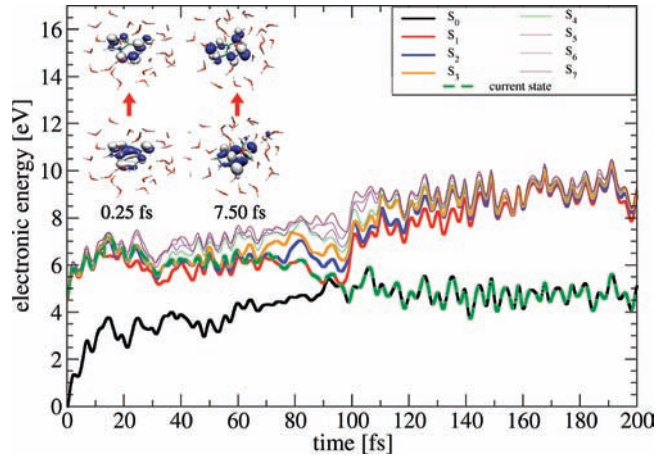

Figure 4. The electronic state energy along a selected nonadiabatic trajectory in microsolvated adenine. The actual state in which the trajectory resides is labeled by the green dashed line. The inset on the left-hand side shows the dominant electronic configurations at 0.25 (π−π^*) and 7.25 fs (n−π^*).

theoretically calculated lifetimes of adenine in the gas phase are significantly shorter than the experimental ones.[32] However, the experimental values are strongly wavelength-dependent and lie in the range between 1.2 and 9 ps (cf. ref 32). For the purpose of comparison, we have also calculated the lifetimes of gas-phase adenine in the frame of TDDFTB. The transition to the ground state is again a two-step process, where the S_2−S_1 transition occurs with the time constant of 120 fs and the S_1−S_0 transition exhibits a time constant of 11 ps. However, the S_1−S_0 transition is strongly wavelength-dependent, which means that it is highly sensitive to quantitative features of the potential energy surfaces, which are difficult to reproduce by available methods. The general trend of the shortening of the lifetime in water is in agreement with the experiments on adenine in solution.[38]

Thus, the nonradiative relaxation of microsolvated adenine occurs in a two-step process, in which, first, the initially excited π−π^* state (S_3) is depopulated on the time scale of 16 fs and, subsequently, the ground state S_0 is populated with the time constant of 200 fs. Notice that the populations of the S_1 and S_2 states grow parallel (cf. Figure 3), and both of them are depopulated as the population of the ground state grows. In Figure 4, we present the electronic state energies along one selected trajectory, showing that in the initial stage of the dynamics, several excited states are very close to the initially excited S_3 state. After the initial excitation to the π−π^* electronic state, within the first 10 fs, the character of the electronic state changes to n−π^* (cf. insets at 0.25 and 7.25 fs in Figure 4). This proximity of electronic states with different character leads to the coupling, which induces several state switchings before the system reaches the S_1 electronic state after ∼75 fs. Subsequently, within ∼25 fs, the crossing with the ground electronic state is reached, and the trajectory continues to propagate in the ground electronic state. The high density of electronic states in microsolvated adenine compared to that in the gas-phase adenine increases the number of pathways which can lead to the crossing with the ground electronic state and thus leads to the shortening for the nonradiative relaxation.

Conclusion

We have presented the combination of the tight binding time-dependent density functional theory (TDDFTB) with the Tully's surface hopping method. This method allows one to extend the

applicability of the TDDFT-based nonadiabatic dynamics into the realm of complex molecular structures and nanostructures due to the high computational efficiency of the TDDFTB approach and the accuracy which is comparable with that of the full TDDFT method.

We have illustrated our approach on the example of the nonradiative relaxation of microsolvated adenine, taking into account the first solvation shell. Our simulations have revealed that the nonradiative transition to the ground electronic state proceeds according to a two-step mechanism involving the ultrafast relaxation of the initially excited $\pi-\pi^*$ state with a lifetime of 16 fs and subsequent transition to the ground state within 200 fs. Overall, the dynamics of microsolvated adenine is thus faster than the one of gas-phase adenine.

Our results demonstrate that the TDDFTB nonadiabatic dynamics represents a useful tool for the investigation of photodynamics in complex systems which are beyond the reach of ab initio methods. This opens the possibility to investigate photoinduced dynamics in systems such as, for example, biochromophores interacting with the protein environments or solvent, light harvesting systems, biosensors, photonic nanoarchitectures, polymers, and so forth. The knowledge of the mechanisms for nonradiative relaxation in these complex systems is mandatory in order to tune their properties for future applications.

Acknowledgment. R. M. acknowledges the financial support in the framework of the DFG Emmy-Noether Program (MI-1236). This work has been supported by the DFG in the framework of the SFB 450. G.S. thanks Thomas Niehaus for helpful discussions and provision of programs.

References and Notes

(1) Michl, J.; Bonačić-Koutecký, V. *Electronic Aspects of Organic Photochemistry*; John Wiley & Sons Inc.: New York, 1990.
(2) *Conical Intersections*; Domcke, W., Yarkony, D. R., Köppel, H., Eds.; World Scientific: Singapore, 2004; Vol. 15.
(3) Robb, M. A.; Garavelli, M.; Olivucci, M.; Bernardi, F. *Rev. Comput. Chem.* **2000**, *15*, 87.
(4) Zewail, A. H. *J. Phys. Chem. A* **2000**, *104*, 5660.
(5) Tully, J. C. *J. Chem. Phys.* **1990**, *93*, 1061.
(6) Hartmann, M.; Pittner, J.; Bonačić-Koutecký, V. *J. Chem. Phys.* **2001**, *114*, 2123.
(7) Mitrić, R.; Bonačić-Koutecký, V.; Pittner, J.; Lischka, H. *J. Chem. Phys.* **2006**, *125*, 024303.
(8) Doltsinis, N. L.; Marx, D. *Phys. Rev. Lett.* **2002**, *88*, 166402.
(9) Craig, C. F.; Duncan, W. R.; Prezhdo, O. V. *Phys. Rev. Lett.* **2005**, *95*, 163001.
(10) Tapavicza, E.; Tavernelli, I.; Rothlisberger, U. *Phys. Rev. Lett.* **2007**, *98*, 023001.
(11) Werner, U.; Mitrić, R.; Suzuki, T.; Bonačić-Koutecký, V. *Chem. Phys.* **2008**, *349*, 319.
(12) Mitric, R.; Werner, U.; Bonačić-Koutecký, V. *J. Chem. Phys.* **2008**, *129*, 164118.
(13) Tapavicza, E.; Tavernelli, I.; Rothlisberger, U.; Filippi, C.; Casida, M. E. *J. Chem. Phys.* **2008**, *129*, 124108.
(14) Granucci, G.; Persico, M.; Toniolo, A. *J. Chem. Phys.* **2001**, *114*, 10608.
(15) Fabiano, E.; Thiel, W. *J. Phys. Chem. A* **2008**, *112*, 6859–6863.
(16) Fabiano, E.; Keal, T. W.; Thiel, W. *Chem. Phys.* **2008**, *349*, 334–347.
(17) Lan, Z.; Fabiano, E.; Thiel, W. *J. Phys. Chem. B* **2009**, *113*, 3548–3555.
(18) Dreuw, A.; Head-Gordon, M. *Chem. Rev.* **2005**, *105*, 4009.
(19) Porezag, D.; Frauenheim, T.; Kohler, T.; Seifert, G.; Kaschner, R. *Phys. Rev. B* **1995**, *51*, 12947–12957.
(20) Seifert, G.; Porezag, D.; Frauenheim, T. *Int. J. Quantum Chem.* **1996**, *58*, 185–192.
(21) Elstner, M.; Porezag, D.; Jungnickel, G.; Elsner, J.; Haugk, M.; Frauenheim, T.; Suhai, S.; Seifert, G. *Phys. Rev. B* **1998**, *58*, 7260–7268.
(22) Frauenheim, T.; Seifert, G.; Elstner, M.; Niehaus, T.; Köhler, C.; Amkreutz, M.; Sternberg, M.; Hajnal, Z.; Di Carlo, A.; Suhai, S. *J. Phys.: Condens. Matter* **2002**, *14*, 3015.
(23) Krueger, T.; Elstner, M.; Schiffels, P.; Frauenheim, T. *J. Chem. Phys.* **2005**, *122*, 114110.
(24) Niehaus, T.; Suhai, S.; Della Salla, F.; Lugli, P.; Elstner, M.; Seifert, G.; Frauenheim, T. *Phys. Rev. B* **2001**, *63*, 5108.
(25) Heringer, D.; Niehaus, T.; Wanko, M.; Frauenheim, T. *J. Comput. Chem.* **2007**, *28*, 2589.
(26) Fabian, J.; Diaz, L.; Seifert, G.; Niehaus, T. *J. Mol. Struct.: THEOCHEM* **2002**, *594*, 41–53.
(27) Improta, R.; Barone, V. *J. Am. Chem. Soc.* **2004**, *126*, 14320.
(28) Gustavsson, T.; Banyasz, A.; Lazzarotto, E.; Markovitsi, D.; Scalmani, G.; Frisch, M.; Barone, V.; Improta, R. *J. Am. Chem. Soc.* **2006**, *128*, 607–619.
(29) Sobolewski, A. L.; Domcke, W.; Ledonder-Lardeux, C.; Jouvet, C. *Phys. Chem. Chem. Phys.* **2002**, *4*, 1093.
(30) Kang, H.; Lee, K. T.; Jung, B.; Ko, Y. J.; Kim, S. K. *J. Am. Chem. Soc.* **2002**, *124*, 12958.
(31) Ullrich, S.; Schultz, T.; Zgierski, M. Z.; Stolow, A. *J. Am. Chem. Soc.* **2004**, *126*, 2262.
(32) Bisgaard, C. Z.; Satzger, H.; Ullrich, S.; Stolow, A. *ChemPhysChem* **2009**, *10*, 101.
(33) Perun, S.; Sobolewski, A. L.; Domcke, W. *J. Am. Chem. Soc.* **2005**, *127*, 6257–6265.
(34) Perun, S.; Sobolewski, A. L.; Domcke, W. *Chem. Phys.* **2005**, *313*, 107.
(35) Blancafort, L.; Cohen, B.; Hare, P. M.; Kohler, B.; Robb, M. A. *J. Phys. Chem. A* **2005**, *109*, 4431.
(36) Serrano-Andres, L.; Merchan, M.; Borin, A. *Proc. Natl. Acad. Sci. U.S.A.* **2006**, *103*, 8691.
(37) Barbatti, M.; Lischka, H. *J. Am. Chem. Soc.* **2008**, *130*, 6831.
(38) Cohen, B.; Hare, P. M.; Kohler, B. *J. Am. Chem. Soc.* **2003**, *125*, 13594.
(39) Jorgensen, W. L.; Chandrasekhar, J.; Madura, J. D.; Impey, R. W.; Klein, M. L. *J. Chem. Phys.* **1983**, *79*, 926–935.
(40) Cornell, W. D.; Cieplak, P.; Bayly, C. I.; Gould, I. R.; Merz, K. M.; Ferguson, D. M.; Spellmeyer, D. C.; Fox, T.; Caldwell, J. W.; Kollman, P. A. *J. Am. Chem. Soc.* **1995**, *117*, 5179–5197.
(41) Becke, A. D. *J. Chem. Phys.* **1993**, *98*, 5648.
(42) Eichkorn, K.; Treutler, O.; Öhm, H.; Häser, M.; Ahlrichs, R. *Chem. Phys. Lett.* **1995**, *240*, 283.
(43) Mennucci, B.; A., T.; Tomasi, J. *J. Am. Chem. Soc.* **2003**, *125*, 13594.

JP905600W